Some Updates and Advertisements

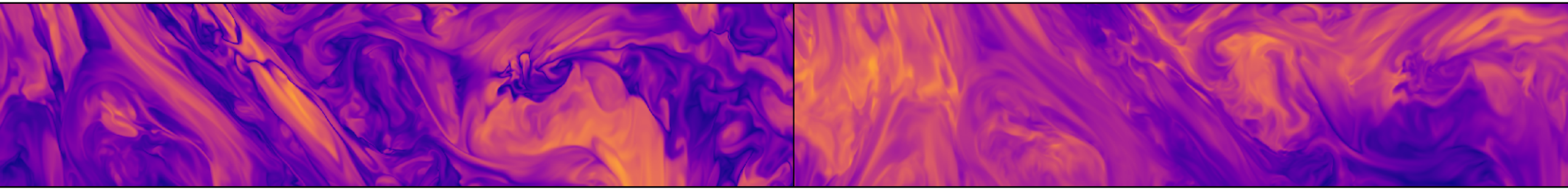

Matthew Kunz

PRINCETON UNIVERSITY

& Lev Arzamasskiy, Archie Bott, Silvio Cerri, Thomas Foster, Alisa Galishnikova, Henrik Latter, Eliot Quataert, Alex Schekochihin, Jono Squire, Denis St-Onge, Wenrui Xu, Evan Yerger, Vladimir Zhdankin

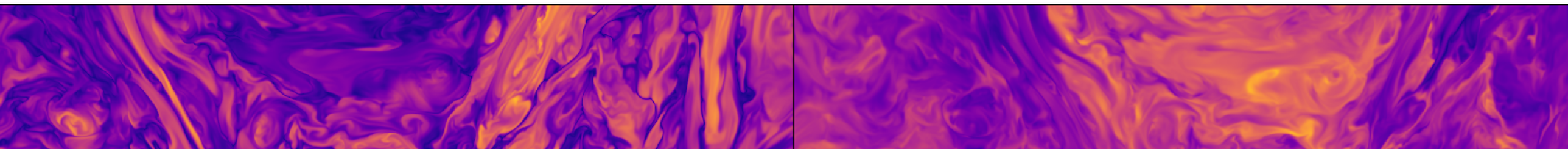

https://www.kitp.ucsb.edu/activities/kinetics24

Interconnections between the Physics of Plasmas and Self-gravitating Systems

Coordinators: Jean-Baptiste Fouvry, Matthew Kunz, Jonathan Squire and Anna Lisa Varri

Scientific Advisors: Alexander Schekochihin and Scott Tremaine

The long-range nature of the inverse square law governs the key physics of both dilute electromagnetic plasmas (i.e. collections of charged particles) and self-gravitating systems (i.e. collections of massive point-like objects in star clusters). This physics is central to understanding many key problems in heliophysics and astrophysics, including the origin of the solar wind, accretion disks around black holes, and star clusters around massive black holes.

The crucial similarity in plasma physics and self-gravitating systems arises from the fact that inter-particle interactions in both systems are primarily governed by coherent forces from distant particles, as opposed to quasi-random forces from violent collisions with nearby particles. This implies they must be described in six-dimensional phase space using kinetic theory. They also exhibit many equivalent processes, such as Landau damping, dynamical friction, resonant relaxation, quasi-periodic orbits, and polarization effects.

However, with a few notable exceptions, the two research communities have remained separate, explaining different phenomena using different languages, across different scales, from different observational data sets. For this program, we aim to stimulate conversation between these two groups, with a particular focus on fundamental kinetic theory such as collisionless/collisional relaxation and phase-space dynamics. The goals are to establish a common language for the kinetic theory of plasmas and self-gravitating systems, to foster a fruitful exchange of ideas and methods between our two communities, and to tackle the fundamental physics of phase-space dynamics in new and creative ways.

Some specific topics and questions for consideration include:

- Collisionless relaxation – how do systems relax in phase space on timescales much shorter than the particle collision time? Do there exist generic relaxed states?
- Collisional relaxation – how do we predict, use, measure, and understand collision operators? What is the impact of finite-N effects?
- Reduced models – how do we formulate and use closures and reduced models (e.g., gyrokinetics or orbit-averaged methods)?
- Stability & Landau damping – how can we compute the dispersion relation and stability of a general kinetic equilibrium?
- Species/mass distributions – how do distributions of particle mass and/or charge change the response of collisionless systems?
- Numerical methods and diagnostics – how can we use numerical simulations to advance theoretical frameworks and to understand their potential pitfalls?

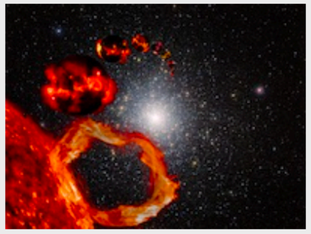

DATES

Jun 3, 2024 - Jul 26, 2024

INFORMATION

Apply

Application deadline is:
Feb 26, 2023.
Primary deadline above date.

Rolling admissions after until the program is filled.

FAMILY SUPPORT INFO

Family Support Info

QUICK LINKS

It's been awhile…

1. Kunz, Squire, Schekochihin & Quataert (2020, JPP)
   Self-sustaining sound in collisionless, high-β plasmas
   P : ion-acoustic waves with $\delta n/n \gtrsim 2/\beta$ generate sufficient pressure anisotropy to trigger firehose and mirror, which scatter and trap particles, thereby impeding the maintenance of Landau resonances that enable such waves' otherwise potent collisionless damping
   Q : *what happens to other kinds of compressive fluctuations?*
   See talk by Stephen Majeski, W morning

It's been awhile…

2. Zhdankin, Uzdensky & Kunz (2021, ApJ)
   Production & persistence of extreme two-temperature plasmas in radiative relativistic turbulence
   P : T_i/T_e grows without bound in turbulent plasmas with inverse Compton cooling of electrons;
   no efficient collisionless mechanisms of electron-ion thermal coupling
   Q : *does this hold at high-β where kinetic instabilities, triggered by pressure anisotropy, could couple ions and electrons?*

It's been awhile…

3. Xu & Kunz (2021ab, MNRAS)

   Formation and evolution of protostellar accretion discs (Parts I & II)

   P : 3D radiative non-ideal MHD simulations of formation and evolution of a young protostellar disc from a magnetized pre-stellar core. Disc becomes gravitationally unstable with prominent large-amplitude spiral arms. Semi-analytic model for the MHD and thermodynamical evolution of the core and disc.

   Q : *Transition to ideal MHD at* $T \gtrsim 1200$ K*?* *Impact of the Hall effect on disc formation?*
   am working with Thomas Foster to better understand magnetic braking in the presence of Hall

   Are most Class 0/I discs gravitationally unstable? seems so — see Wenrui Xu (2022, MNRAS)

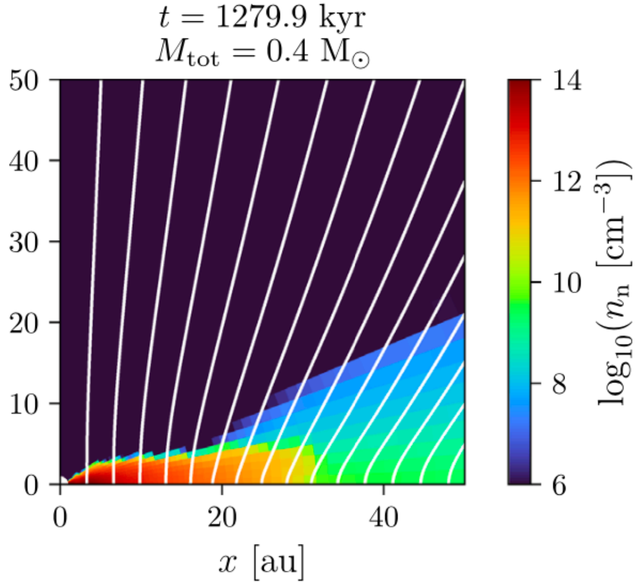

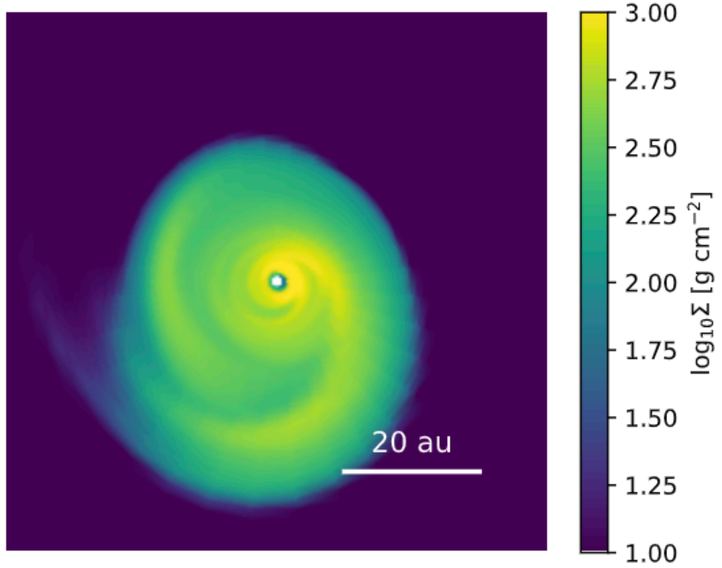

It's been awhile…

4. Cerri, Arzamasskiy & Kunz (2021, ApJ)
   On stochastic heating and its phase-space signatures in low-β kinetic turbulence
   P : Dominant contribution to stochastic heating of ions in low-β kinetic turbulence is ***not*** from the $E \times B$ potential. Obtained scaling relations for particle-energization rate and energy diffusion coefficient in AWs/KAWs. Diagnosed phase-space signatures of ion heating using `Pegasus++` simulations, showing Landau damping, ion-cyclotron heating, stochastic heating, and intermittency effects. Matched theory. Cautions on quantitative inference of stochastic heating in solar wind.
   Q : *How do these processes manifest in imbalanced turbulence?*

Most recently…

5. Latter & Kunz (2022, MNRAS)

   The vertical shear instability in poorly ionized, magnetized protoplanetary discs

   P : local linear theory that explores how non-ideal MHD influences the VSI, while exciting additional diffusive shear instabilities (à la Kunz 2008). VSI likely operational inside ~ 10 au.

   Q : *Interaction with gravitational instability (if present)? Differential settling of dust grains? Nonlinear evolution?*

6. Arzamasskiy, Kunz, Squire, Quataert & Schekochihin (2022, submitted; arXiv:2207.05189)

   Kinetic turbulence in collisionless high-β plasmas

   P : Interplay between local wave-wave interactions (cascade) and non-local wave-particle interactions (firehose, mirror). Effective viscosity is large in critically balanced Alfvénic turbulence. Mostly ion heating (80-90%) by viscous damping. Steep kinetic-energy spectrum.

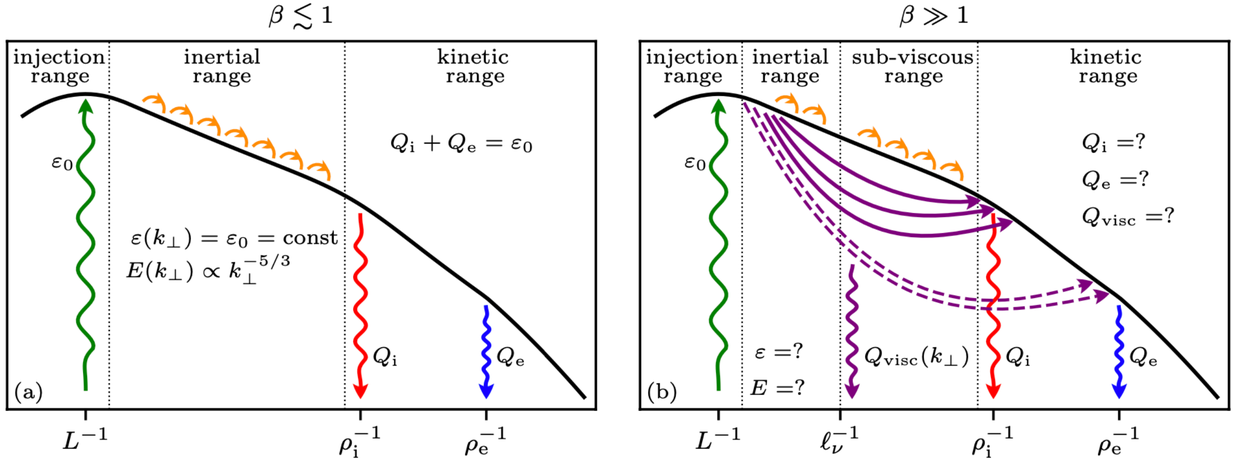

Most recently…

7. Galishnikova, Kunz & Schekochihin (2022, nearly accepted by PRX)
   Tearing instability and current-sheet disruption in the turbulent dynamo
   P : Pm $\gtrsim 1$, Rm $\gg 1$ turbulent dynamo produces folds susceptible to resistive tearing. Predicted "tearing scale" matches well characteristic field-reversal scale in high-resolution MHD simulations. Sub-tearing steepening of magnetic spectrum to a slope consistent with that predicted for tearing-mediated Alfvénic turbulence. Spectral peak is ~independent of resistive scale

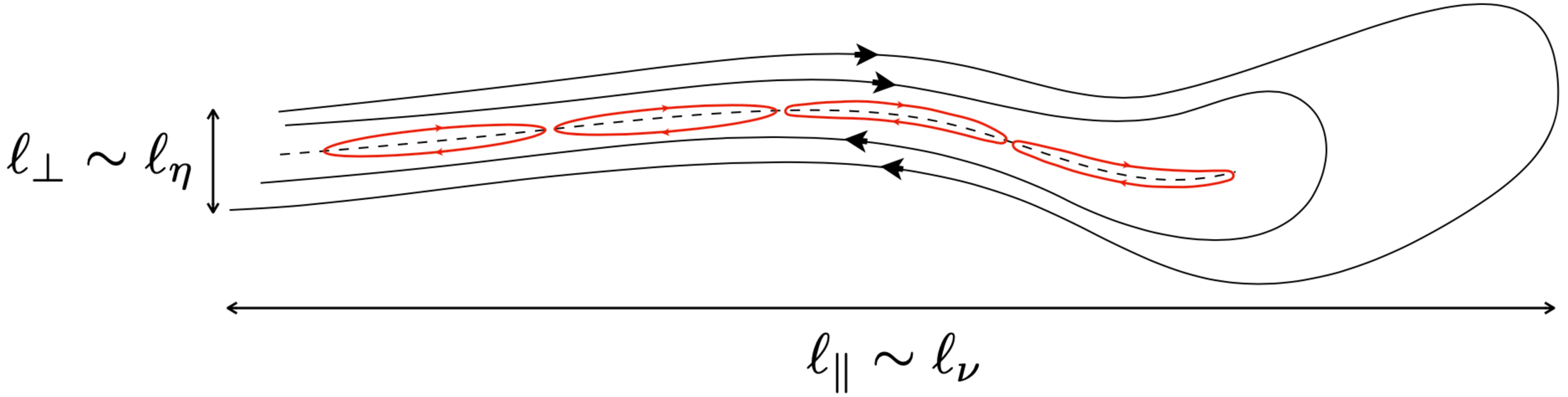

Performed large parameter study
of $\mathrm{Pm} \gtrsim 1$ MHD dynamo
up to highest resolutions

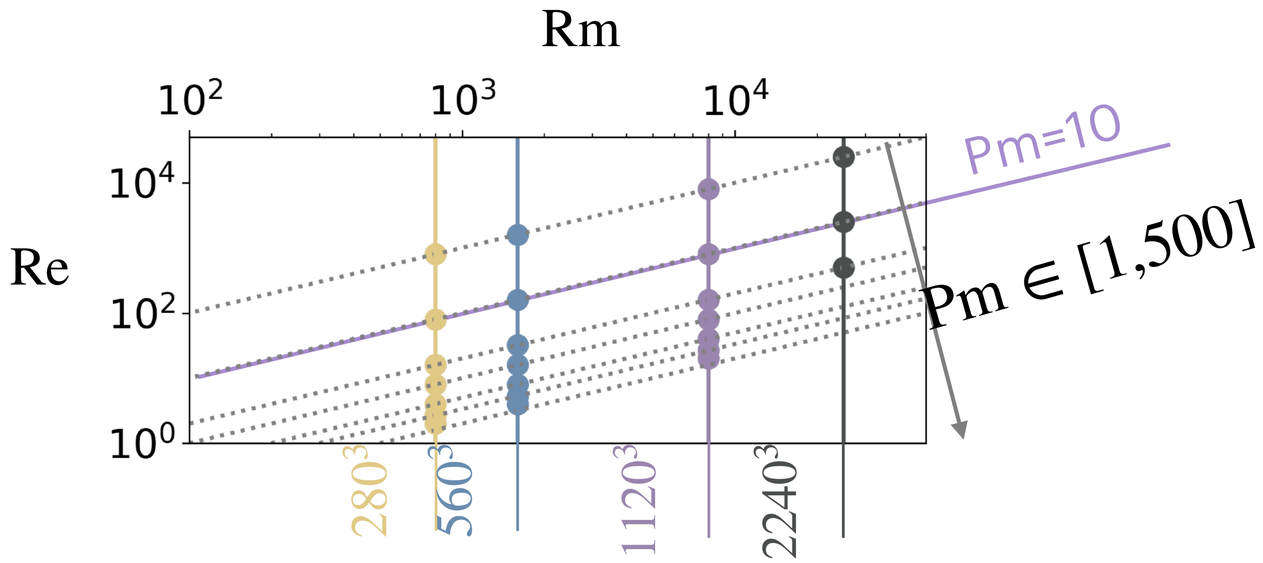

increasing resolution

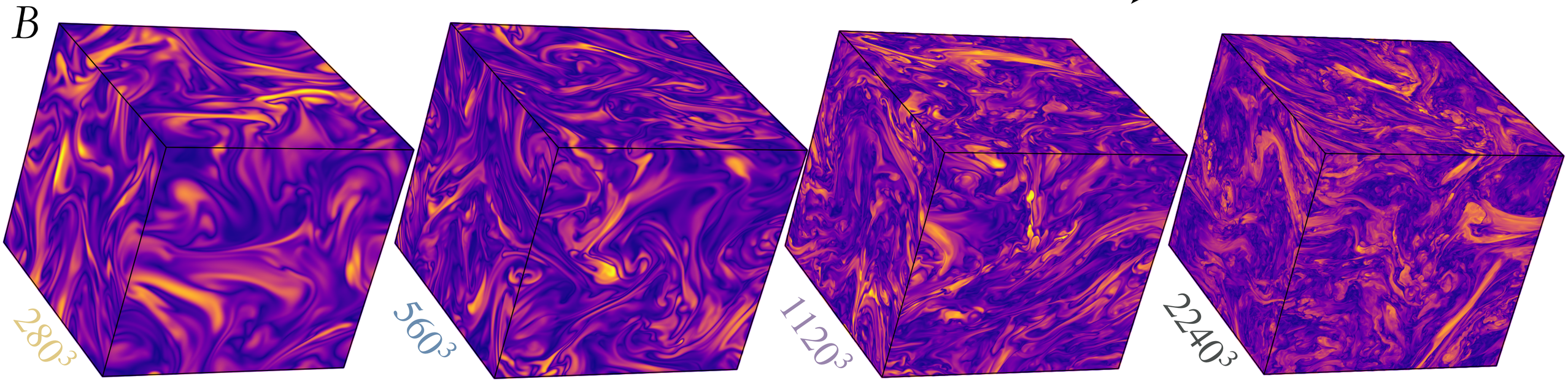

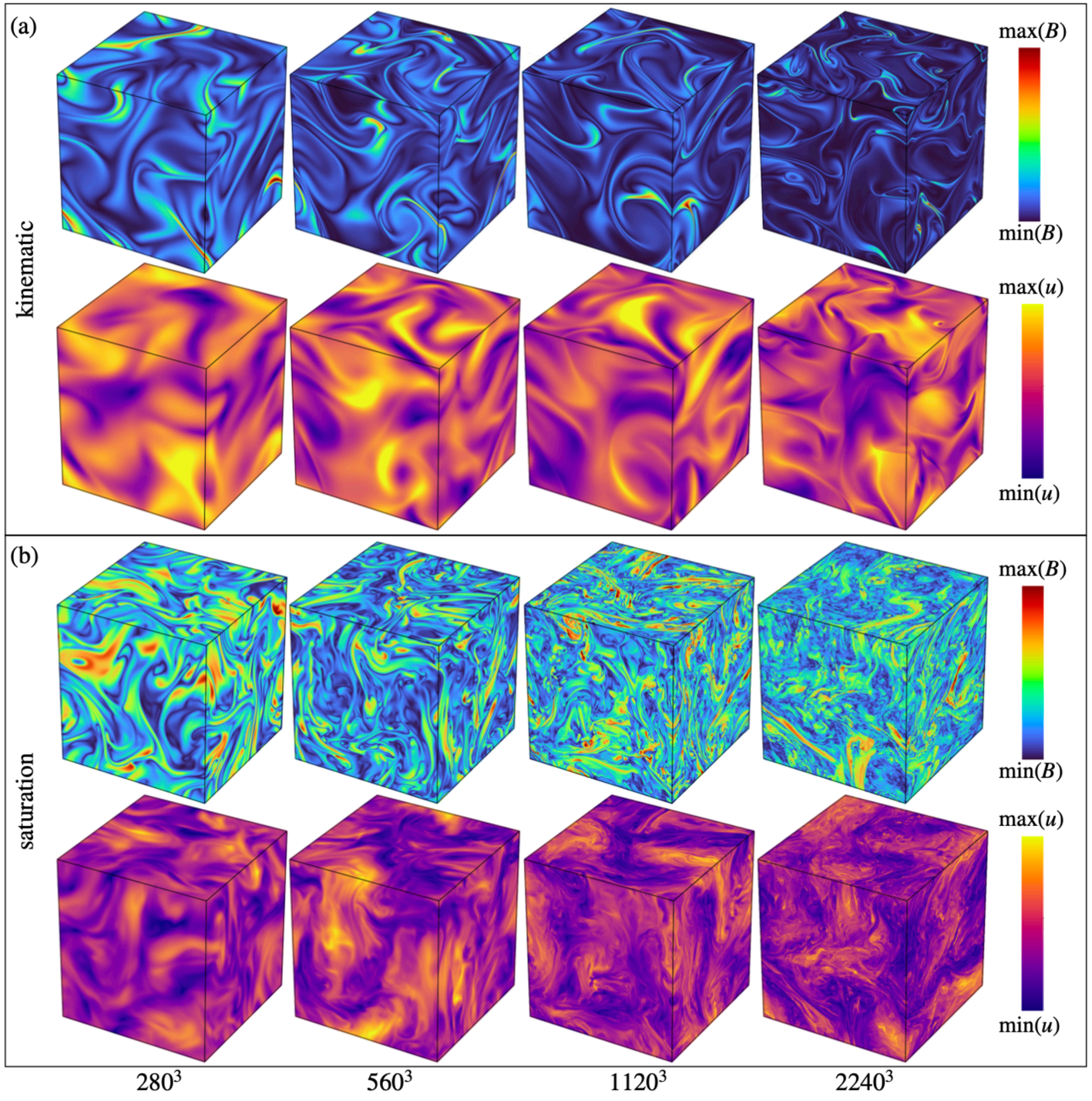

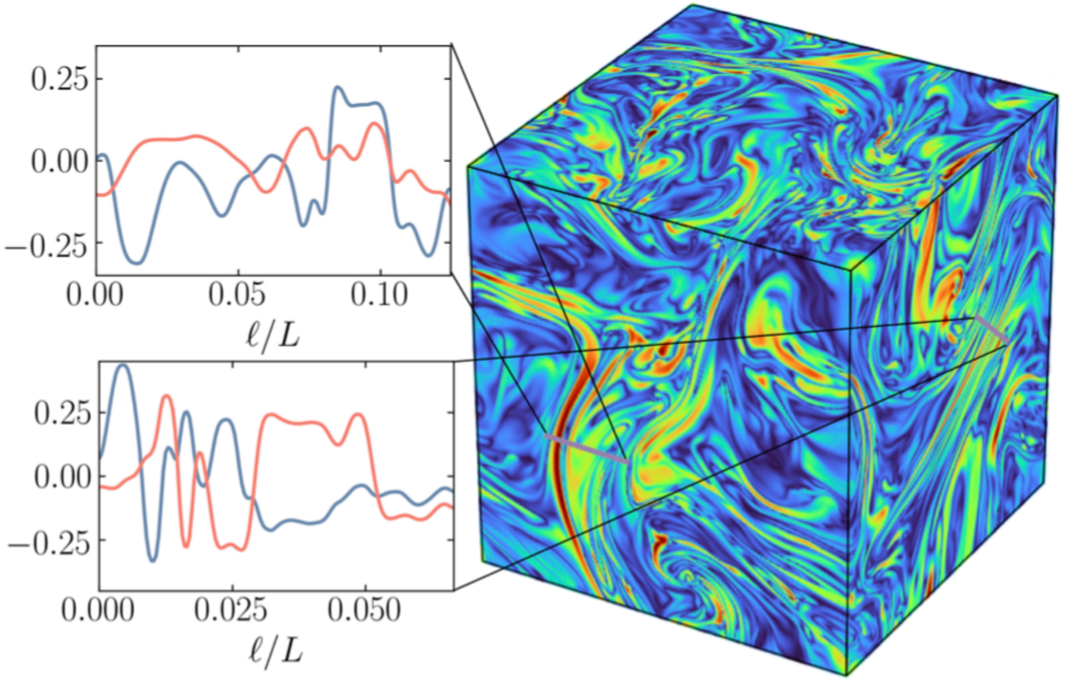

FIG. 3. Snapshot of magnetic-field strength in the saturated state of run c7 (1120^3, Pm = 500, Re ≈ 20, Rm ≈ 10^4). Large Pm results in elongated laminar current sheets, in contrast to those seen in run c2 (1120^3, Pm = 10, Re ≈ 10^3, Rm ≈ 10^4; see Figure 2a). Two 1D spatial cuts of the magnetic field are shown on the left side; colors indicate different projections of the magnetic field: in-plane (blue) and out-of-plane (red).

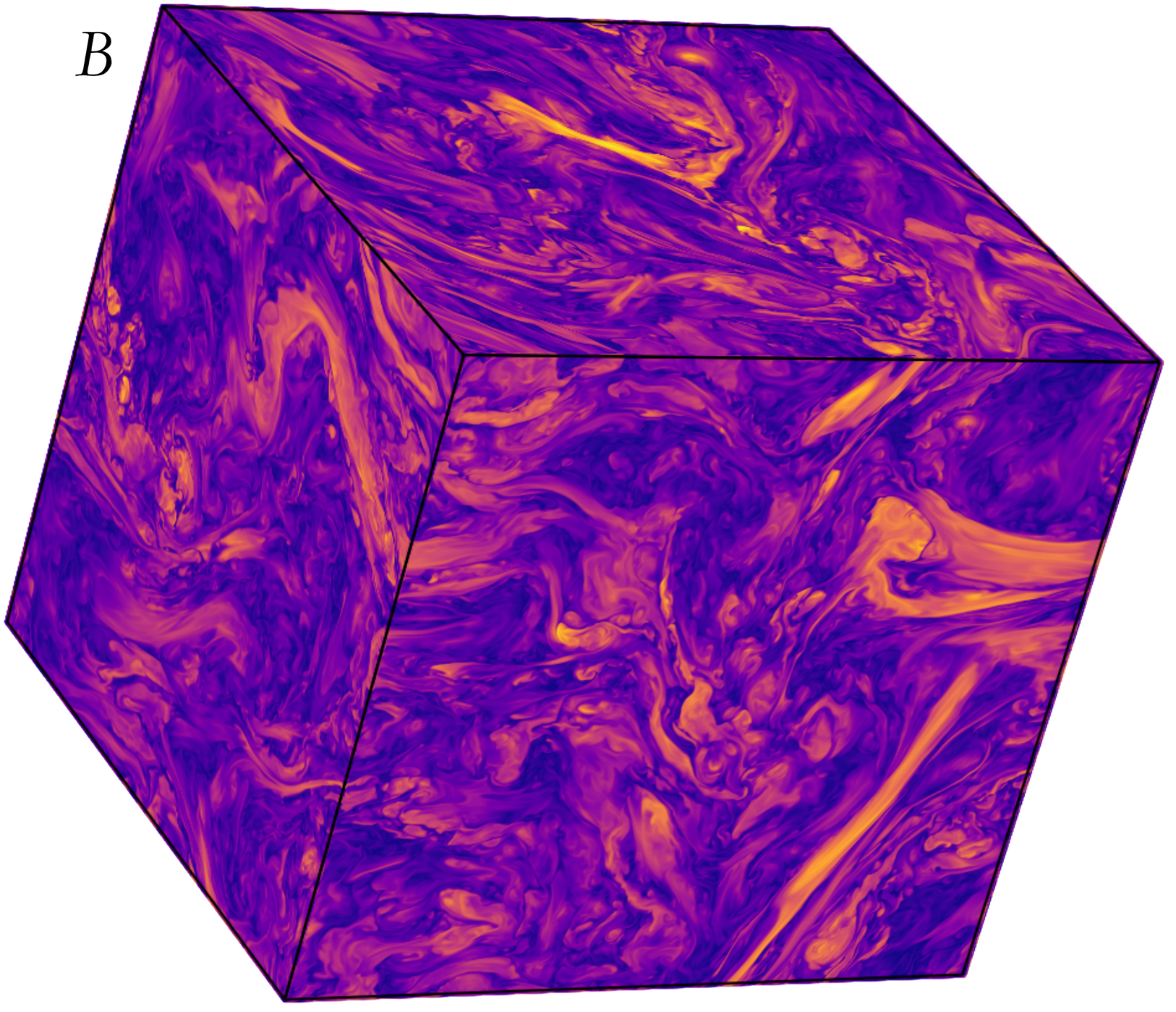
B

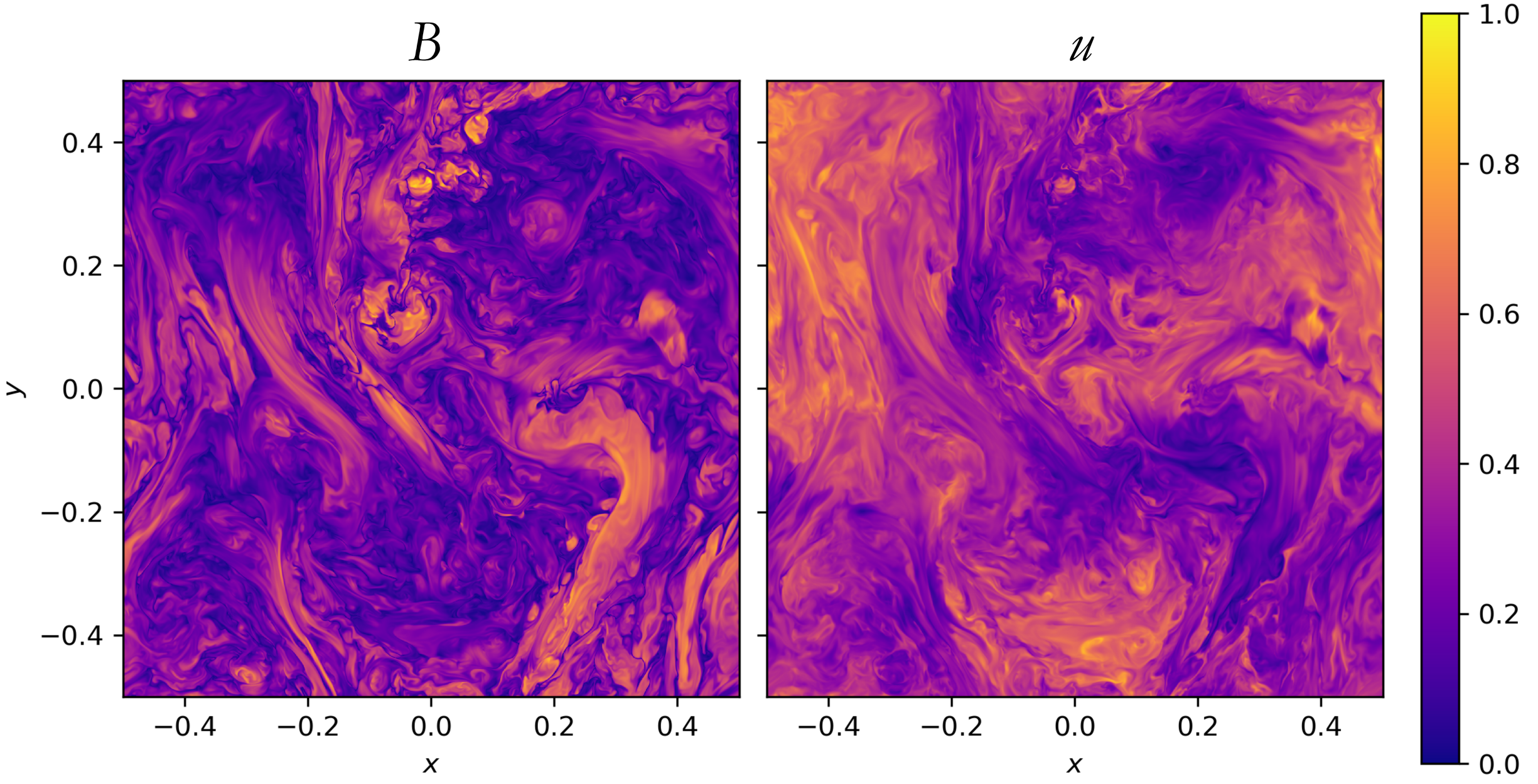
at 2240³, Pm = 10
B
u
0.4
0.2
0.0
−0.2
−0.4
y
−0.4
−0.2
0.0
0.2
0.4
x
1.0
0.8
0.6
0.4
0.2
0.0

$|\boldsymbol{J}|$

at 2240^3, Pm = 10

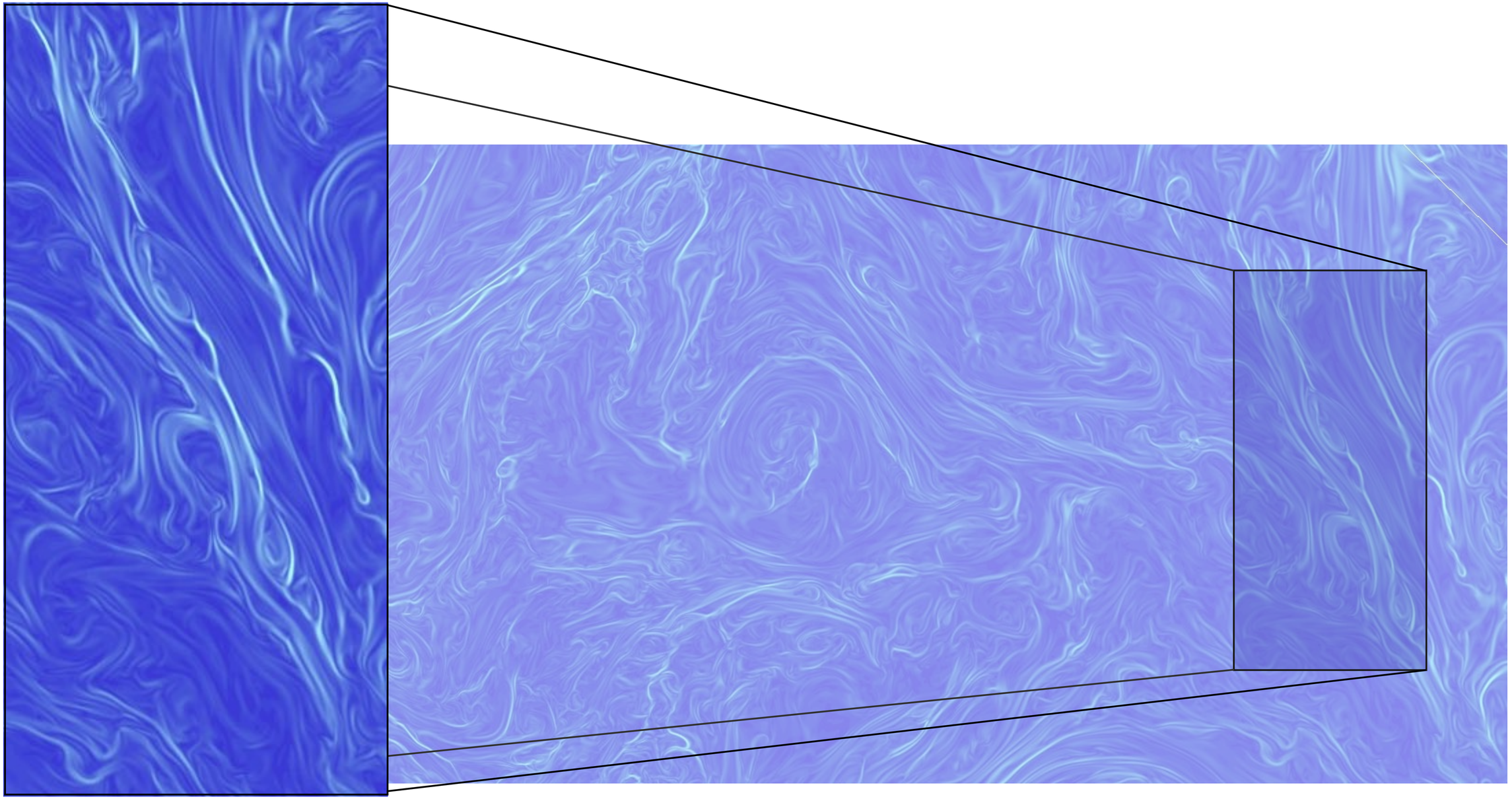

at 2240^3, Pm = 10

visual evidence for tearing of magnetic folds and "plasmoids"

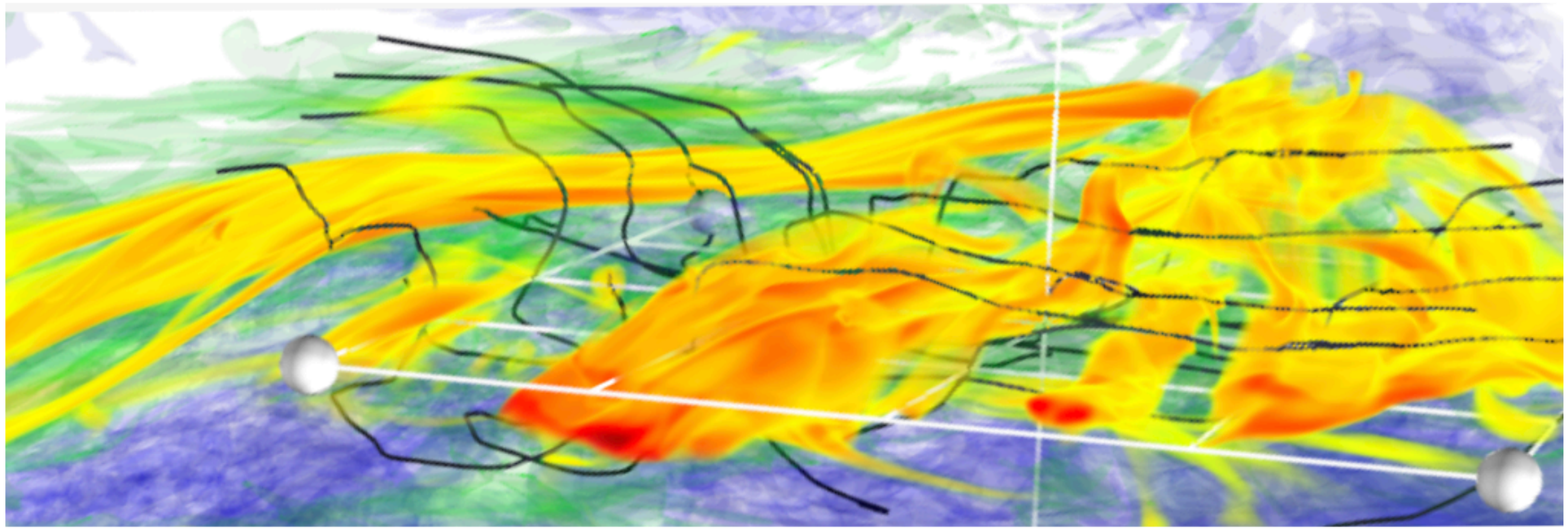

magnetic-field lines

field strength

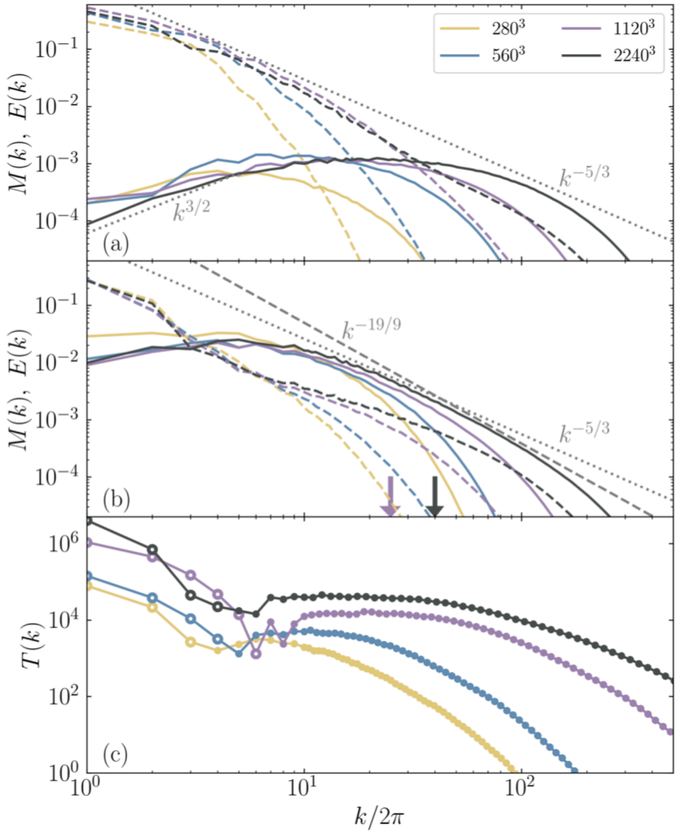

FIG. 5. Angle-integrated spectra for Pm = 10 at different resolutions (runs a2, b2, c2, and d2). Color coding of lines is the same in all panels. (a) Kinetic $E(k)$ (dashed) and magnetic $M(k)$ (solid) energy spectra at the end of the kinematic stage, normalized by $\rho_0 u_{\rm rms,sat}^2$. The spectral peak of the magnetic energy depends on the resolution. (b) Kinetic $E(k)$ (dashed) and magnetic $M(k)$ (solid) energy spectra, normalized by $\rho_0 u_{\rm rms,sat}^2$, time-averaged over the saturated state. The arrows indicate the predicted field-reversal scale λ_*^{-1} [see Eq. (10a)] for Pm = 10 at 1120^3 (purple) and 2240^3 (black). The magnetic-energy spectrum acquires a slope steeper than $-5/3$ starting at $k/2\pi \sim \lambda_*^{-1}$, which at 2240^3 is consistent with the spectral envelope of $k^{-19/9}$ expected for a tearing-mediated cascade. The spectral peak of the magnetic energy appears to be independent of Rm. (c) Transfer function $T(k)$ in saturation, normalized by $\rho_0 u_{\rm rms,sat}^3$, with filled (open) circles corresponding to work done by (against) the Lorentz force.

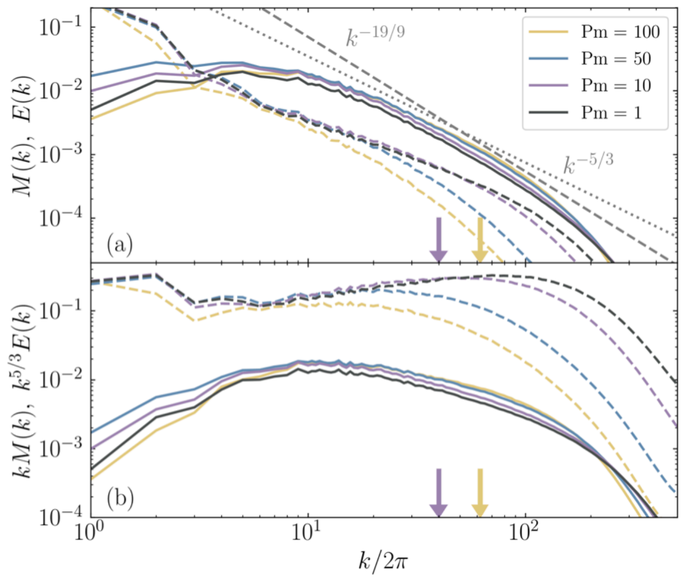

FIG. 6. (a) Angle-integrated kinetic $E(k)$ (dashed) and magnetic $M(k)$ (solid) spectra, time-averaged over the saturated state of runs d1, d2, d3, and d4 (2240^3 at different Pm), normalized by $\rho_0 u_{\rm rms,sat}^2$. The magnetic-energy spectrum steepens to be consistent with the predicted $-19/9$ envelope for a tearing-mediated cascade at a wavenumber that increases slightly with Pm; cf. Eq. (10a), which predicts $\lambda_*^{-1} \propto {\rm Pm}^{1/5}$ at fixed Rm when $n = 2$. The arrows indicate the predicted λ_*^{-1} for Pm = 10 (purple) and 100 (yellow). (b) Kinetic spectra, compensated by $k^{5/3}$, and magnetic spectra, compensated by k, to illustrate the argument made at the end of §III D; here $kM(k)$ is multiplied by an arbitrary factor of 0.1 to separate it visually from the other curves.

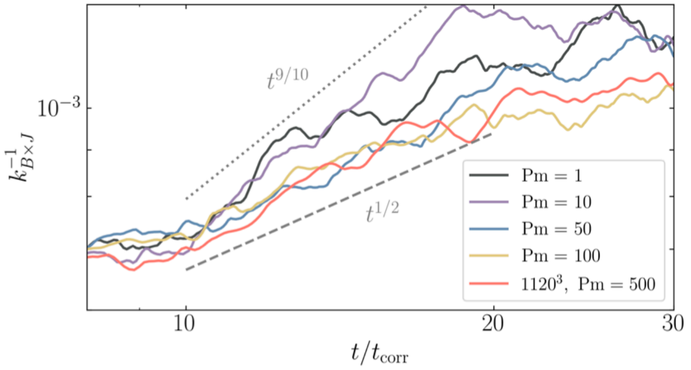

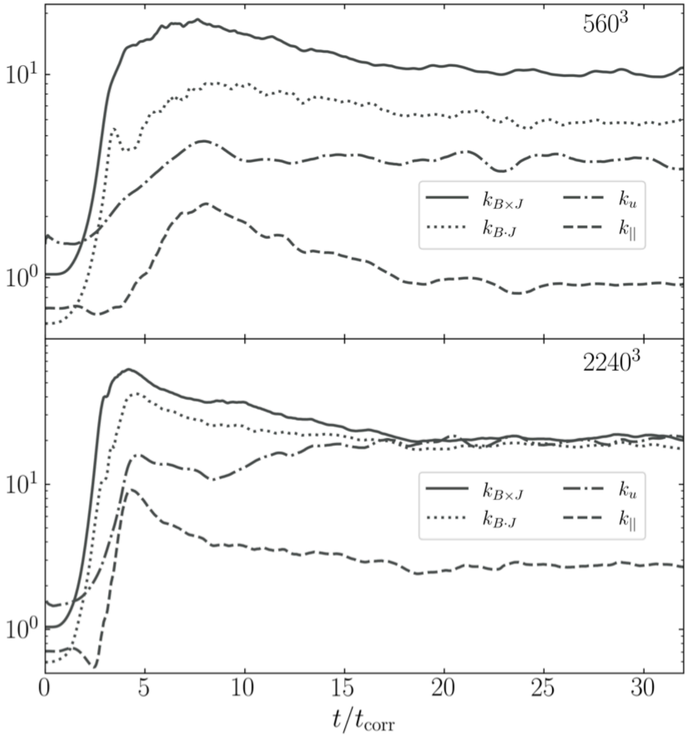

FIG. 9. Time evolution of the characteristic wavenumbers $(k_\parallel, k_{B\cdot J}, k_{B\times J})$ describing the magnetic field [see Eq. (19)] and k_u describing the small-scale structure of the velocity field [see Eq. (20)] at Pm = 10 and resolutions 560^3 and 2240^3.